

## Article

# Novel Antioxidant Peptides Identified from *Arthrospira platensis* Hydrolysates Prepared by a Marine Bacterium *Pseudoalteromonas* sp. JS4-1 Extracellular Protease

Congling Liu <sup>1,†</sup>, Gong Chen <sup>1,†</sup>, Hailian Rao <sup>1</sup>, Xun Xiao <sup>1</sup>, Yidan Chen <sup>1</sup>, Cuiling Wu <sup>2</sup>, Fei Bian <sup>3,\*</sup> and Hailun He <sup>1,\*</sup> 

<sup>1</sup> State Key Laboratory of Medical Genetics, School of Life Sciences, Central South University, Changsha 410013, China

<sup>2</sup> Department of Biochemistry, Changzhi Medical College, Changzhi 046000, China

<sup>3</sup> Institute of Crop Germplasm Resources, Shandong Academy of Agricultural Sciences, Jinan 250100, China

\* Correspondence: bxf.9@163.com (F.B.); helenhe@csu.edu.cn (H.H.); Tel.: +86-531-6665-9499 (F.B.); +86-0731-8265-0230 (H.H.)

† These authors contributed equally to this work.

**Abstract:** Crude enzymes produced by a marine bacterium *Pseudoalteromonas* sp. JS4-1 were used to hydrolyze phycobiliprotein. Enzymatic productions showed good performance on DPPH radical and hydroxyl radical scavenging activities ( $45.14 \pm 0.43\%$  and  $65.11 \pm 2.64\%$ , respectively), especially small peptides with MWCO <3 kDa. Small peptides were fractioned to four fractions using size-exclusion chromatography and the second fraction (F2) had the highest activity in hydroxyl radical scavenging ability ( $62.61 \pm 5.80\%$ ). The fraction F1 and F2 both exhibited good antioxidant activities in oxidative stress models in HUVECs and HaCaT cells. Among them, F2 could upregulate the activities of SOD and GSH-Px and reduce the lipid peroxidation degree to scavenge the ROS to protect *Caenorhabditis elegans* under adversity. Then, 25 peptides total were identified from F2 by LC-MS/MS, and the peptide with the new sequence of INSSDVQGKY as the most significant component was synthesized and the ORAC assay and cellular ROS scavenging assay both illustrated its excellent antioxidant property.

**Keywords:** phycobiliprotein; antioxidant peptide; bacterial extracellular protease; enzymatic hydrolyzation; *C. elegans*



**Citation:** Liu, C.; Chen, G.; Rao, H.; Xiao, X.; Chen, Y.; Wu, C.; Bian, F.; He, H. Novel Antioxidant Peptides Identified from *Arthrospira platensis* Hydrolysates Prepared by a Marine Bacterium *Pseudoalteromonas* sp. JS4-1 Extracellular Protease. *Mar. Drugs* **2023**, *21*, 133. <https://doi.org/10.3390/md21020133>

Academic Editors: Elena Talero and Javier Ávila-Román

Received: 30 December 2022

Revised: 16 February 2023

Accepted: 16 February 2023

Published: 20 February 2023



**Copyright:** © 2023 by the authors. Licensee MDPI, Basel, Switzerland. This article is an open access article distributed under the terms and conditions of the Creative Commons Attribution (CC BY) license (<https://creativecommons.org/licenses/by/4.0/>).

## 1. Introduction

The microalgae *Arthrospira* belongs to the cyanobacteria division, the cyanophyceae class, and the Oscillatoriaceae family. *Arthrospira* sp. is a photosynthetic cyanobacterium that has recently grown in value as a nutritional supplement and food additive due to its high protein content of around 60–70% in their biomass and various valuable natural compounds, such as pigments,  $\beta$ -carotenes, polysaccharides and peptides. In addition, *Arthrospira* sp. has a wide range of uses in the pharmaceutical, cosmetic, and nutritional industries. Because of its high protein content and nutritive value of amino acid composition, *Arthrospira* sp. was evaluated as a potential meat substitute and has received increased attention [1]. Phycobiliprotein is a class of proteins with antioxidant, antitumor and anti-inflammatory properties, but the heat sensitivity and allergenicity limit its wider applications. Phycobiliprotein is highly abundant in *Arthrospira*, accounting for about 20% of its dry weight [2]. Using proteases to hydrolyze the phycobiliprotein to produce antioxidant peptides is an efficient way to reach higher bioactive potential and promote high value utilization of marine proteins while avoiding its natural limitations. Moreover, the proteins of microalgae can be converted by enzymatic hydrolysis into value-added products with better functional properties such as antioxidant peptides (APs), anti-hypertension peptides,

and antibacterial peptides, etc. Therefore, more and more researchers are interested in obtaining effective bioactive peptides (BPs) from *Arthrospira* sp. hydrolysates.

Enzymatic hydrolysis of the dietary proteins generates BPs, which are short chains of 2–15 amino acids residues, can enhance nutritional value, safety, bioactive function and reduce the allergenicity [3,4]. Numerous studies have demonstrated that BPs with antioxidant activity produced by proteolysis can achieve antioxidation by scavenging free radicals, chelating transition metals, and enhancing the activity of endogenous antioxidant enzymes such as catalase (CAT), superoxide dismutase (SOD), and glutathione peroxidase (GSH-Px). Redox homeostasis (balance) is an important cellular process that plays a vital role in maintaining the normal physiological steady state of the human body. A disturbance of balance between oxidants and antioxidants results in oxidative stress. Reactive oxygen species (ROS) are molecules derived from aerobic cellular metabolism; in the oxidative stress condition excessive production of ROS can disrupt the intracellular redox balance and cause numerous diseases such as cancer, diabetes, atherosclerosis, cardiovascular and neurodegenerative [4]. A growing number of studies have demonstrated that APs from protease hydrolysates can effectively scavenge free radicals or inhibit the production of ROS. Meanwhile, food-derived APs also performed nontoxicity, are low cost, absorb efficiency advantages, and were considered as potential substitutes for commercial synthetic antioxidants [5,6].

Since different proteases have specific hydrolyzed performance on protein substrate and can produce diverse BPs with different length, sequence, and composition, these hydrolyzes may exhibit various hydrophobicity and functionalities [7,8]. Therefore, it is necessary to find a new enzymes resource to hydrolyze *Arthrospira platensis* (*A. platensis*) and produce novel APs with high antioxidant activity and bioactive properties. Our previous study suggested using extracellular proteases secreted by a marine bacterium *Pseudoalteromonas* sp. JS4-1 to hydrolyze *Chlorella* can obtain hydrolysates with high antioxidant activity [9]. In this study, proteases from *Pseudoalteromonas* sp. JS4-1 were used to hydrolyze *A. platensis* proteins and produced diverse APs; a series of biochemical assays, cell models, and animal models were applied for testing the bioactivity of the APs.

## 2. Results

### 2.1. Screening of Proteases for Enzymatic Hydrolysis

*Pseudoalteromonas* is a strictly marine genus and able to produce extracellular enzymes, which have good advantages in degrading natural marine proteins [10]. In order to evaluate which enzyme is more suitable for hydrolyzing *Arthrospira* sp. proteins, the extracellular enzymes from eight strains named *Pseudoalteromonas* sp. B27-3, *Pseudoalteromonas* sp. B47-6, *Pseudoalteromonas* sp. B62-3, *Pseudoalteromonas* sp. WH05-1, *Pseudoalteromonas* sp. WH06-2, *Pseudoalteromonas* sp. WH16-2, *Pseudoalteromonas* sp. JS4-1 and *Pseudoalteromonas* sp. ZB23-2 were extracted and screened by zymography. The enzymatic hydrolysates were identified by SDS-PAGE and their DPPH RSA and OH RSA activities were also detected. The zymography showed with the exception of *Pseudoalteromonas* sp. WH06-2 and *Pseudoalteromonas* sp. WH16-2, all the other strains can secrete a variety of proteases, indicating that most marine bacteria could produce extracellular proteases with a variety of cleavage sites, and suitable for enzymatic hydrolysis (Figure 1A). Proteases from *Pseudoalteromonas* sp. B27-3 and *Pseudoalteromonas* sp. JS4-1 have stronger hydrolysis activity than other bacterial proteases toward *Arthrospira* sp. proteins. SDS-PAGE showed that the hydrolysates existed in smaller fragments compared with the control protein, and almost no protein band left on the gel, while the hydrolysates produced by other bacterial proteases still left visible bands on the gel (Figure 1B). The hydrolysates of *Pseudoalteromonas* sp. JS4-1 proteases have the highest DPPH RSA ( $45.14 \pm 0.43\%$ ) and OH RSA ( $65.11 \pm 2.64\%$ ) than other productions (Figure 1C,D). Therefore, proteases from *Pseudoalteromonas* sp. JS4-1 were selected as a candidate for *Arthrospira* sp. proteins hydrolyzing.

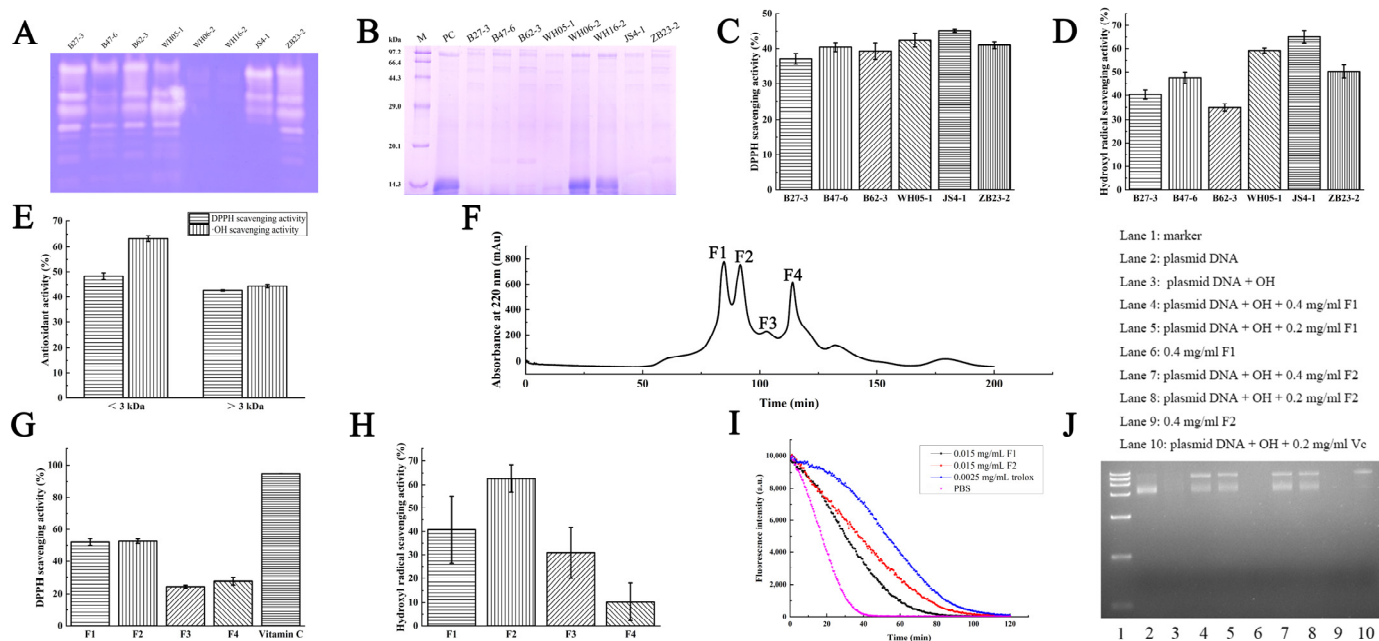


**Figure 1.** Antioxidant activities of phycobiliprotein hydrolysis products with JS4-1. (A) Comparison of catalytic ability on casein of proteases from *Pseudoalteromonas* sp. B27-3, *Pseudoalteromonas* sp. B47-6, *Pseudoalteromonas* sp. B62-3, *Pseudoalteromonas* sp. WH05-1, *Pseudoalteromonas* sp. WH06-2, *Pseudoalteromonas* sp. WH16-2, *Pseudoalteromonas* sp. JS4-1 and *Pseudoalteromonas* sp. ZB23-2. (B) SDS-PAGE electrophoresis of phycobiliprotein and hydrolysates of different proteases (Line M: protein marker, Line PC: phycobiliprotein). (C) DPPH radical and (D) hydroxyl radical scavenging activity of phycobiliprotein hydrolysates of different proteases. (E) Antioxidant activities of the ultrafiltration fraction of phycobiliprotein hydrolysis products treated with optimized hydrolysis condition. Data were expressed as mean  $\pm$  SD ( $n = 3$ ). (F) Size-exclusion liquid chromatography of the <3 kDa ultrafiltration fractions on a Sephadex LH-20 column. The F1–F4 represent purified fractions. (G) DPPH radical scavenging activity of F1–F4 compared with Vitamin C. (H) Hydroxyl radical scavenging activity of F1–F4. (I) Peroxyl radical scavenging activity (ORAC) of F1 and F2 compared with PBS and Trolox. (J) Protective effects of F1 and F2 on hydroxyl radical-induced oxidation of plasmid DNA compared with Vitamin C. Data were expressed as mean  $\pm$  SD ( $n = 3$ ).

## 2.2. Optimization of Enzymatic Hydrolyzing Parameters

Enzymatic hydrolyzation was optimized using the one-variable-at-a-time (OVAT) approach by changing one parameter while keeping other parameters constant. First, the hydrolyzing was performed at 50 °C from 1 h to 7 h with 1 h at intervals, at a E: S ratio of 1:10, to estimate the optimal hydrolyzing time. Data showed that the hydrolysis degree increased along with the hydrolyzing process, especially in the initial three hours. After five hours hydrolyzation, the hydrolysis degree was not improved significantly. DPPH RSA as an evaluation index suggested that when the E/S ratio ranged from 1:6 to 1:10, the DPPH RSA of the hydrolytes exhibited no significant difference. While the E/S ratio adjusted to 1:12 and 1:14, the DPPH RSA of the hydrolytes dropped 6.72% and 15.95%, respectively, indicating that the substrate exceeded the catalytic capacity of the enzymes. When the hydrolyzing temperature increased, the DPPH RSA improved and reached the maximal activity at 50 °C, but when the temperature exceeded >50 °C the DPPH RSA decreased, probably due to the enzymes being inactivated at higher temperatures. After OVAT optimization, when E:S ratio was 1:10 and enzymatic hydrolyzing performed at 50 °C for 4 h, the DPPH RSA and the OH RSA of the hydrolysates achieved the maximal level of  $48.51 \pm 2.42\%$  and  $67.16 \pm 3.21\%$ , respectively. The ninhydrin colorimetry was used to determine the hydrolysis degree, and data showed that about  $0.67 \pm 0.02$  mM of  $\bullet\text{NH}_2$  was released after hydrolyzing reaction.

In order to evaluate the free RSA of small peptides, the hydrolysates were separated into 2 parts by ultrafiltration. The DPPH RSA of < 3 kDa and > 3 kDa parts were  $48.26 \pm 1.34\%$  and  $42.60 \pm 0.25\%$ , respectively. The OH RSA of < 3 kDa and > 3 kDa parts were  $63.30 \pm 1.11\%$  and  $44.30 \pm 0.68\%$ , respectively (Figure 1E). It has been proven that the small peptides (<3 kDa) contained more antioxidant components and were more easy to exert biological effects [11]. The bioactive peptides with small molecular weight have broad application potential in food, medicine, cosmetics and other industries due to their good absorbability and fewer side effects besides their higher bioactivity [12].

### 2.3. Antioxidant Activities of Size-Exclusion Liquid Chromatography Fractions of Phycobiliprotein Hydrolysis Products

In order to investigate the antioxidant components of the small peptides, the peptides with MWCO <3 kDa were further separated using size-exclusion liquid chromatography, and in total four fractions defined as F1 to F4 were obtained (Figure 1F). By measuring the DPPH RSA (F1 to F4 were  $52.06 \pm 2.13\%$ ,  $52.56 \pm 1.38\%$ ,  $24.43 \pm 0.85\%$  and  $27.58 \pm 2.24\%$ , respectively; Figure 1G) and the OH RSA (F1 to F4 were  $40.75 \pm 14.35\%$ ,  $62.61 \pm 5.80\%$ ,  $30.86 \pm 10.90\%$ , and  $10.21 \pm 7.91\%$ , respectively; Figure 1H), F1 and F2 showed higher antioxidant activity than F3 and F4. We could obtain about 40 mg of F1 and 40 mg of F2 lyophilized powder after the size-exclusion liquid chromatography from 1 g of *A. Platensis* powder.

Then, the ORAC assay was performed to compare the antioxidant activity of F1 and F2. At peptide concentration of 0.015 mg/mL, both F1 and F2 could significantly slow down the decrease rate of the fluorescence decay compared with PBS. The Trolox equivalent antioxidant capacity of F1 and F2 were  $0.27 \pm 0.02$  mmol TE/g and  $0.41 \pm 0.04$  mmol TE/g, respectively (Figure 1I). F2 exhibited higher antioxidant activity than F1.

The hydroxyl radicals could open the circular of supercoiled DNA (SC DNA) and make it become partly opened circular DNA (OC DNA), which can slow down the DNA mobility on agarose gel. Comparing with the no damaged plasmid DNA pET-22b (Figure 1J, lane 2), when the plasmid DNA has no protection, it can be completely degraded by hydroxyl radicals into small fragments and no band observed on the gel (Figure 1J, lane 3). An amount of 0.2 mg/mL of Vitamin C can protect the plasmid DNA from oxidative damage, but the protection is limited and the OC DNA is the major form retained on the gel (Figure 1J, lane 10). F1 and F2 concentrations range from 0.2 mg/mL to 0.4 mg/mL; all can significantly protect plasmid DNA from oxidative damage and these protections were far better than Vitamin C, which make the SC DNA and OC DNA co-existing on the gel (Figure 1J, lane 4, 5, 7, 8). So, this study proved that both F1 and F2 have strong antioxidant activity to protect DNA from oxidative stress.

### 2.4. Antioxidant Activities of F1 and F2 at Cellular Levels

The intracellular oxidized cell model is a common method that is used to assess the antioxidative capacity of compounds. Vascular endothelial cell injury is associated with several factors, among them oxidative stress is an important cause of cardiovascular disease. APs are able to protect vascular endothelial cell function which is a key point in the prevention and treatment for cardiovascular diseases. The skin is the first immune defense of the body and susceptible to a variety of physical and chemical stimuli. Protecting skin cells could be an effective strategy to prevent and treat dermatosis. Therefore, we chose HUVECs and HaCaT cells as cellular models to investigate the intracellular antioxidant effects of F1 and F2 [13–16].

MTT assay indicated that both F1 and F2 had no significant cytotoxicity on HUVECs and HaCaT cells; moreover, they can obviously increase the cell viability at a concentration range of 100–500 µg/mL (Figure 2A,B and Figure 3A,B).

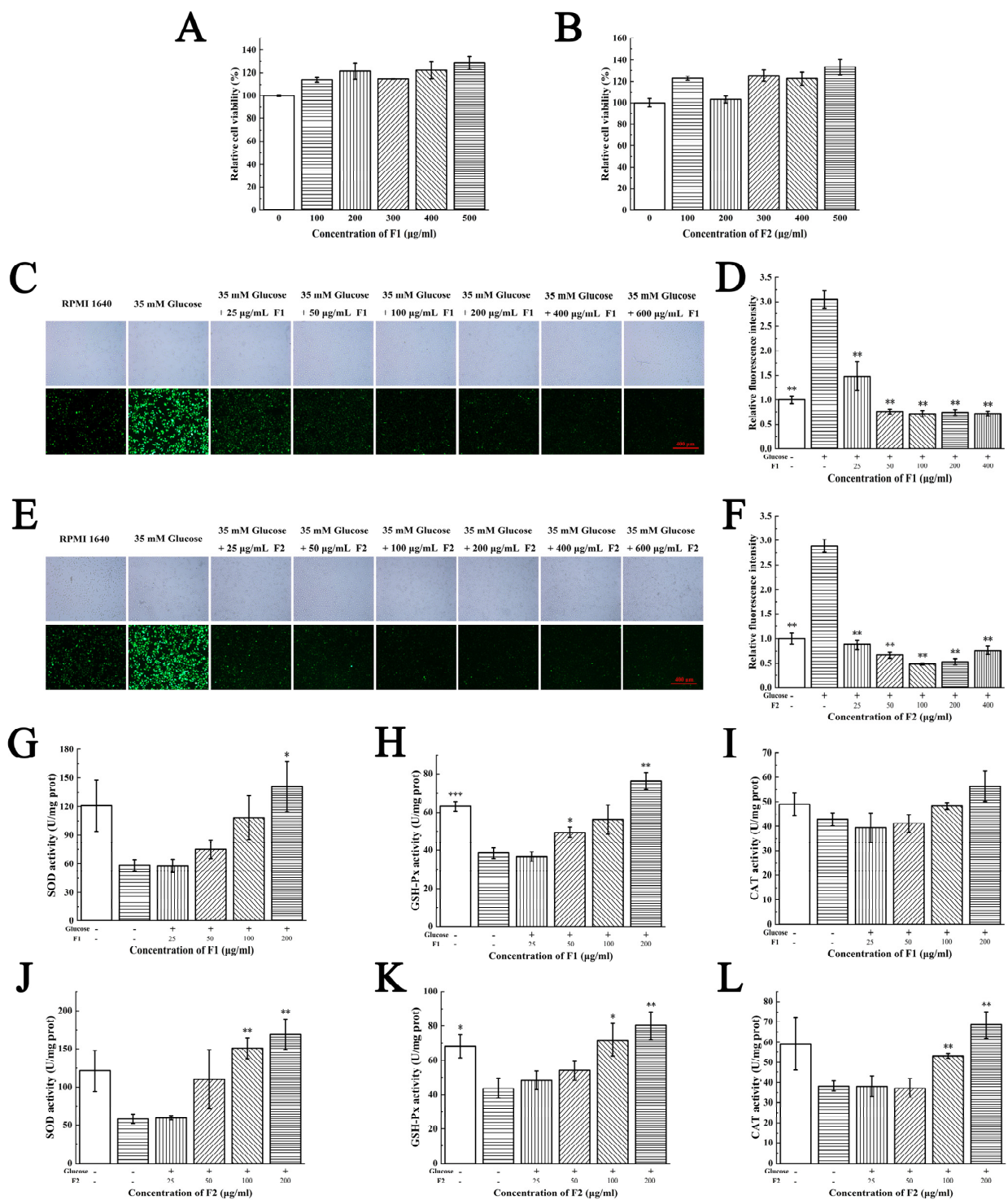


**Figure 2.** Antioxidant activities of F1 and F2 on HUVEC cells. The effects of different concentration of (A) F1 and (B) F2 on cell viability were measured by MTT assay. ROS scavenging capacities of (C) F1 and (E) F2 on HUVEC cells indicated as a green DCFH-DA fluorescence. Images were taken using fluorescence microscope (magnification, 10×). (D,F) Statistical analysis was performed to quantify relative fluorescence density accordingly (Student *t*-test). (G,J) Superoxide dismutase (SOD), (H,K) glutathione peroxidase (GSH-Px) and (I,L) catalase (CAT) activities in HUVEC cells were detected after treatment with F1 and F2, respectively. The Normality of data was analyzed by Shapiro–Wilk test. Data were expressed as mean ± SD (*n* = 3). \* represents *p* < 0.05, \*\* represents *p* < 0.01 and \*\*\* represents *p* < 0.001, compared with glucose group (Student *t*-test).

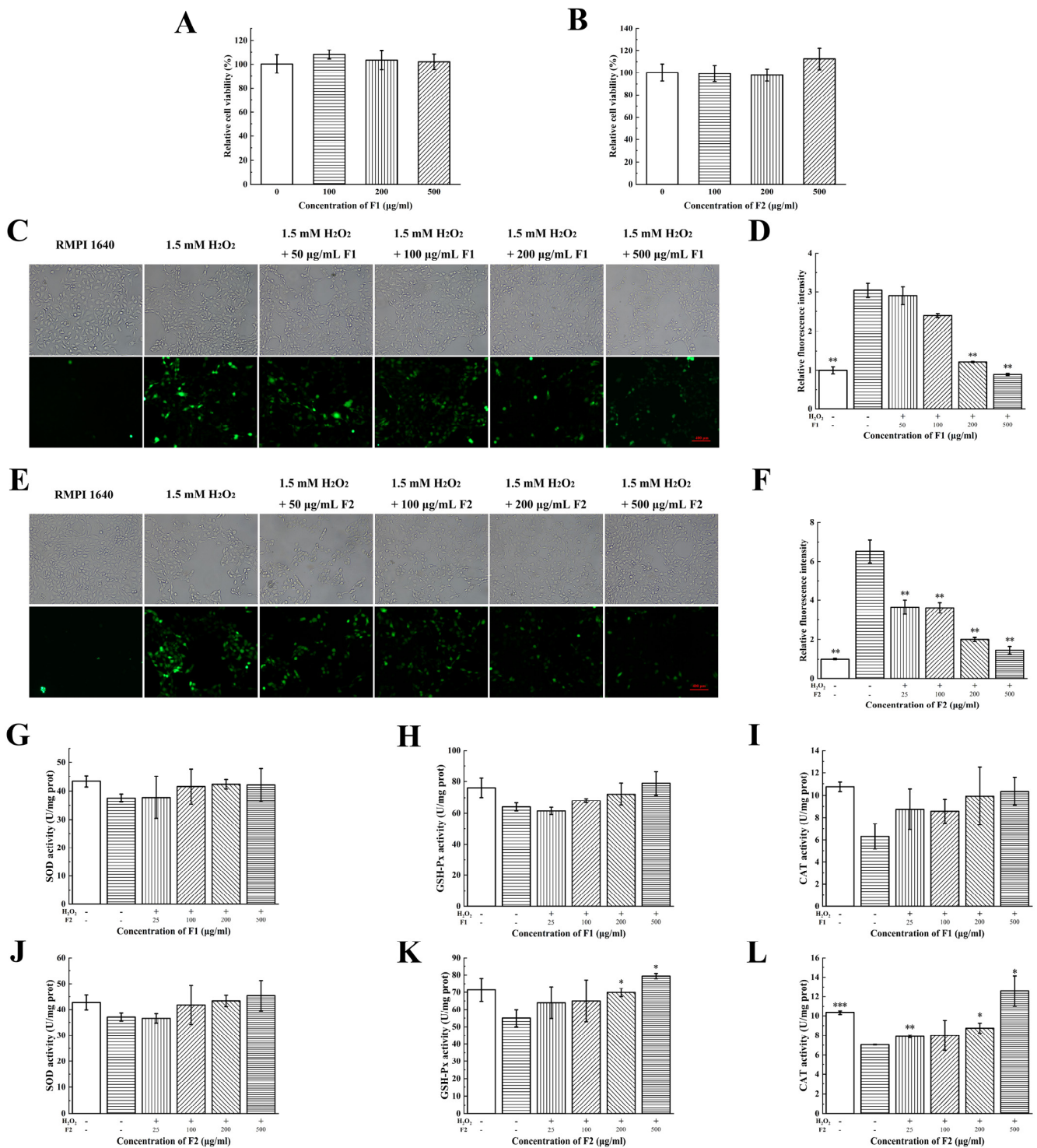


**Figure 3.** Antioxidant activities of F1 and F2 on HaCaT cells. The effects of different concentration of (A) F1 and (B) F2 on cell viability were measured by MTT assay. ROS scavenging capacities of (C) F1 and (E) F2 on HaCaT cells indicated as green DCFH-DA fluorescence. Images were taken using fluorescence microscope (magnification, 10×). (D,F) Statistical analysis was performed to quantify relative fluorescence density accordingly (Student *t*-test). (G,J) Superoxide dismutase (SOD), (H,K) glutathione peroxidase (GSH-Px) and (I,L) catalase (CAT) activities in HaCaT cells were detected after treatment with F1 and F2, respectively. The Normality of data was analyzed by Shapiro–Wilk test. Data were expressed as mean ± SD (*n* = 3). \* represents *p* < 0.05, \*\* represents *p* < 0.01 and \*\*\* represents *p* < 0.001, compared with H<sub>2</sub>O<sub>2</sub> group (G,J Mann–Whitney test; H,I,K,L Student *t*-test).

An amount of 35 mM of glucose was added to the HUVECs and 1.5 mM H<sub>2</sub>O<sub>2</sub> was used in the HaCaT cells. Cells treated with glucose and H<sub>2</sub>O<sub>2</sub> exhibited higher fluorescence intensity than control groups, indicating the oxidative stress models have been successfully established (Figure 2C,E and Figure 3C,E). The intracellular ROS were labelled by DCFH-DA probe. Cells treated with low concentration of F1 and F2 (25 µg/mL) displayed less fluorescence intensity than the glucose group in HUVECs, suggesting the fractions were able to scavenge intracellular ROS to protect HUVECs from hyperglycemia-induced oxidative stress (Figure 2D,F). Cells treated with a high concentration of F1 (100 µg/mL) and a low concentration of F2 (50 µg/mL) displayed less fluorescence intensity than the H<sub>2</sub>O<sub>2</sub> group in HaCaT cells, suggesting that the fractions were able to scavenge intracellular ROS to protect HaCaT cells from H<sub>2</sub>O<sub>2</sub> induced oxidative stress (Figure 3D,F). The antioxidant activities of peptides on a cellular level in this study were close to those reported extracts of plants [17–19], which suggested the peptides in our study may also have great potential applications.

To further investigate the underlying mechanisms of fractions scavenging intracellular ROS, we detected the activities of antioxidant enzymes such as SOD, GSH-Px and CAT after being treated with fractions due to their role in scavenging ROS and suppressing oxidative stress [20,21]. The glucose and H<sub>2</sub>O<sub>2</sub> reduced the activities of SOD, GSH-Px and CAT in HUVECs and HaCaT cells. The administration of F1 and F2 dose-dependently increased the activities of these enzymes at a concentration range of 25–200 µg/mL (Figure 2G–L and Figure 3G–L).

#### 2.5. Effects of F2 on Resistance to Oxidative Stress in *C. elegans*

*Caenorhabditis elegans* (*C. elegans*) have many highly conserved genes and signaling pathways involved in the regulation of aging and oxidative stress [22,23]. The genes and pathways in aging, oxidative stress and inflammation between *C. elegans* and human are highly homologous [24]. *C. elegans* as an animal model is widely used for anti-aging and anti-oxidative studies.

In this study, 0.5 mg/mL of F1 and F2 had no toxicity and no significant life-extending effect on N2 (Figure 4A). The in vivo ROS assay showed that 0.5 mg/mL of F1 had no significant ROS scavenging effects, while F2 could scavenge ROS at low concentration (0.2 mg/mL, Figure 4E,F). The fluorescence accumulation assay of 80 nematodes showed similar results (Figure 4G).

Then, we speculate whether the APs can enhance the stress resistance of N2. Oxidizing agent H<sub>2</sub>O<sub>2</sub> (10 mM), pesticide paraquat (10 mM) and heat (35 °C) were chosen as stress conditions. Considering F2 has higher anti-oxidative activity than F1, in this study N2 were treated with F2 and then exposed to stress conditions. Data showed that the F2 can extend the stressed N2 survival time in all stress conditions, and the survival rate was positively correlated with the addition of F2. An amount of 0.2 mg/mL of F2 increased 35% survival rate after 7 h of H<sub>2</sub>O<sub>2</sub> stress, 50% after 120 h of paraquat stress and 24% under heat stress (Figure 4B–D). Although F2 did not help the *C. elegans* live longer, it really improved the resistant ability of *C. elegans* obviously to the oxidation, pesticide and heat stress.

We then investigated the MDA levels and activities of antioxidant enzymes in nematodes. The MDA level is an important biomarker of lipid peroxidation [25]. F2 could significantly reduce the MDA levels in nematodes (Figure 4H). As shown in Figure 4I–K, F2 could have dose-dependently increased the activities of SOD and GSH-Px, while it had no effects on CAT. These results suggested that F2 could upregulate the activities of SOD and GSH-Px and reduce the lipid peroxidation degree to scavenge the ROS in the organisms. Activating these antioxidant enzymes contributes to maintaining the redox balance, delaying aging process and prolonging lifetime [26]. Antioxidant enzymes with high activity are able to reduce ROS levels, maintain normal physiological steady state and prevent numerous diseases such as cancer, diabetes, neurodegenerative diseases and so on [4].

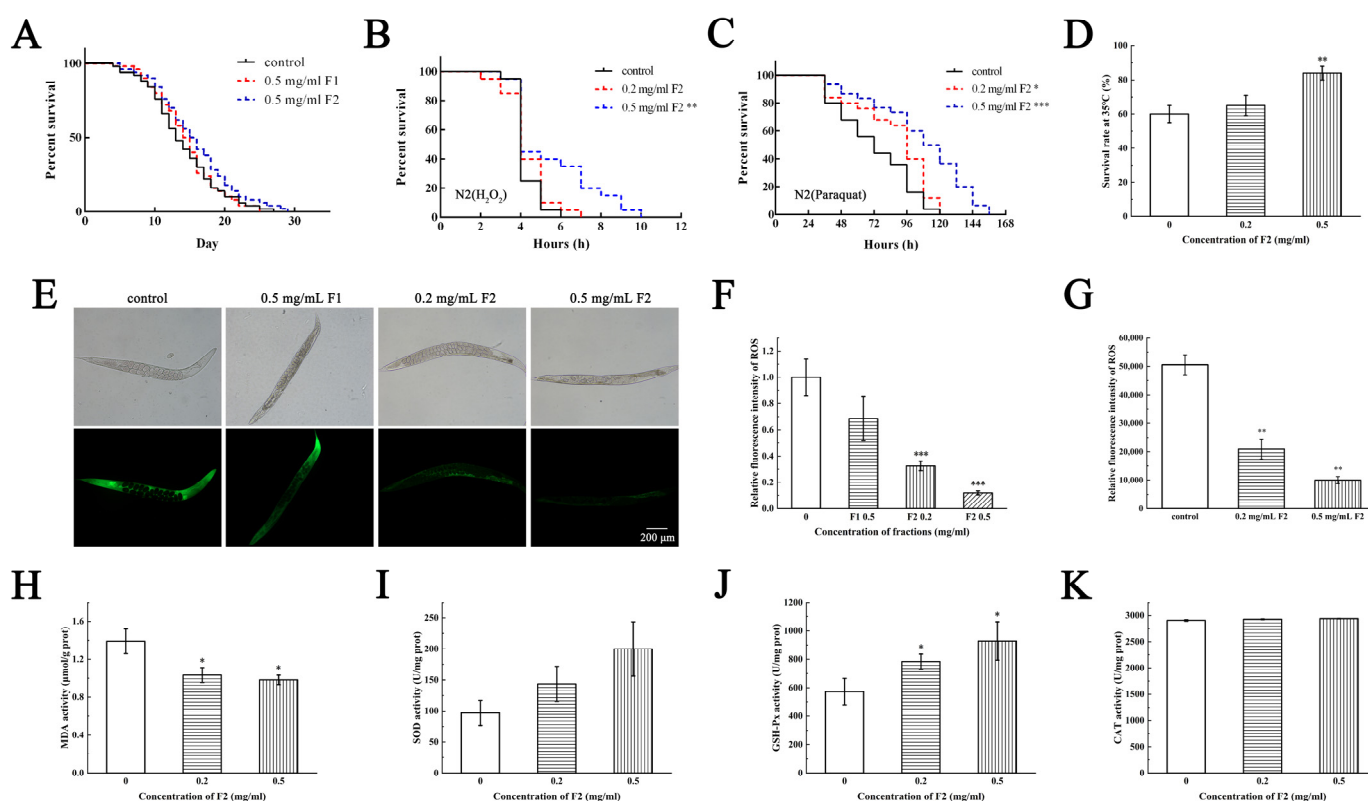


**Figure 4.** Effects of F2 on resistance to oxidative stress in *Caenorhabditis elegans*. (A) Survival curves of *C. elegans* treated with F1 and F2. Survival curves of *C. elegans* pre-treated with F2 at given concentrations for 3 days and then exposed to (B) 10 mM  $H_2O_2$  and (C) 10 mM paraquat. \* represents  $p < 0.05$ , \*\* represents  $p < 0.01$  and \*\*\* represents  $p < 0.001$ , compared with  $H_2O_2$  and paraquat group (Student *t*-test). (D) Survival rate of *C. elegans* pre-treated with F2 at given concentrations for 3 days and then cultured at 35 °C for 10 h. (E) Antioxidant activities of F2 on *C. elegans* were detected by DCFH-DA probe. Images were taken using fluorescence microscope (magnification, 5 $\times$ ). (F) Statistical analysis was performed to quantify relative fluorescence density (Student *t*-test). (G) The ROS content in *C. elegans* was determined based on the average integrated area of the fluorescence intensity of probes during 6 h intervals. (H) MDA levels, (I) superoxide dismutase (SOD), (J) glutathione peroxidase (GSH-Px) and (K) catalase (CAT) activities in *C. elegans* were detected after treated with F2 for 3 days. The Normality of data was analyzed by Shapiro–Wilk test. Data were expressed as mean  $\pm$  SD ( $n = 3$ ). \* represents  $p < 0.05$ , \*\* represents  $p < 0.01$  and \*\*\* represents  $p < 0.001$ , compared with blank control group (Student *t*-test).

## 2.6. Antioxidant Activities of Synthesized Peptide INSSDVQGKY

Since F2 has the highest antioxidant activity in all fractions, its components were investigated using LC-MS/MS. The total ion chromatography of F2 was shown in Figure S1. A total of 25 peptides with relative abundance  $>1\%$  were identified, and their sequence and abundance were listed in Table 1. Among them, one peptide with the sequence of INSSDVQGKY accounting for 17.83% was considered as the major component of F2. The MS/MS of INSSDVQGKY was shown in Figure S2.

**Table 1.** Peptides identified through liquid chromatography mass spectrum (> 1%).

| Amino Acid Sequence | Mass (Da) | Source (Position)   | Counts (%) |
|---------------------|-----------|---|------------|
| INSSDVQGKY          | 1109.535  | Allophycocyanin beta-subunit [ <i>Arthrospira platensis</i> qy3] (9–18)                   | 17.83      |
| VGGSVPREY           | 962.482   | Elongation factor G [ <i>Arthrospira platensis</i> ] (531–539)                            | 9.12       |
| SSYPNRPVP           | 1015.509  | Photosystem II lipoprotein Psb27 [ <i>Arthrospira platensis</i> C1] (102–110)             | 8.81       |
| GIFDTMNH            | 933.401   | ATP-dependent Clp protease proteolytic subunit [ <i>Arthrospira platensis</i> C1] (74–81) | 6.91       |
| YTPDYTPK            | 983.460   | Ribulose biphosphate carboxylase large chain [ <i>Arthrospira platensis</i> C1] (26–33)   | 3.34       |
| IDPSHGTGF           | 929.424   | Phospho-2-dehydro-3-deoxyheptonate aldolase [ <i>Arthrospira platensis</i> ] (277–285)    | 3.33       |
| TPEPKPEPKPEPKPEP    | 1795.936  | CAAD domain-containing protein [ <i>Arthrospira platensis</i> C1] (52–67)                 | 3.25       |
| YEQMPEPKY           | 1183.522  | NAD(P)H-quinone oxidoreductase subunit K [ <i>Arthrospira platensis</i> C1] (105–113)     | 3.14       |
| DVDWSDYQKQ          | 1282.547  | Ferredoxin-NADP reductase [ <i>Arthrospira platensis</i> ] (380–389)                      | 2.78       |
| VGGSVPKEY           | 934.476   | Elongation factor G [ <i>Arthrospira platensis</i> C1] (496–504)                          | 2.76       |
| TDVPANHPY           | 1012.461  | S-layer domain protein [ <i>Arthrospira platensis</i> C1] (283–291)                       | 2.42       |
| QGTLEKYI            | 950.507   | Putative adenylate cyclase [ <i>Arthrospira platensis</i> C1] (375–382)                   | 2.40       |
| AGIDEINRT           | 987.499   | Phycocyanin alpha-subunit [ <i>Arthrospira platensis</i> qy3] (113–121)                   | 2.32       |
| SESPNLILMDIQMP      | 1586.768  | Multi-sensor hybrid histidine kinase [ <i>Arthrospira platensis</i> C1] (1700–1713)       | 2.32       |
| APYDESEVVFH         | 1291.572  | Rod linker polypeptide CpcI [ <i>Arthrospira platensis</i> ] (107–117)                    | 2.20       |
| IDTIPTGGK           | 900.492   | 50S ribosomal protein L13 [ <i>Arthrospira platensis</i> C1] (144–152)                    | 1.96       |
| LIAGGTGPM           | 815.421   | Phycocyanin alpha-subunit [ <i>Arthrospira platensis</i> qy3] (99–107)                    | 1.92       |
| DVDWSDYQK           | 1154.488  | Ferredoxin-NADP reductase [ <i>Arthrospira platensis</i> ] (380–388)                      | 1.90       |
| LPEEPMTGK           | 1000.490  | Transcriptional regulator AbrB family [ <i>Arthrospira platensis</i> C1] (9–17)           | 1.80       |
| VINSSDVQGKY         | 1208.604  | Allophycocyanin beta-subunit [ <i>Arthrospira platensis</i> qy3] (8–18)                   | 1.68       |
| LVTQQPLGGKAQ        | 1238.698  | DNA-directed RNA polymerase subunit beta [ <i>Arthrospira platensis</i> ] (992–1003)      | 1.52       |
| KELTKKSPNSP         | 1227.682  | NYN domain-containing protein [ <i>Arthrospira platensis</i> ] (398–408)                  | 1.37       |
| IETKEIPVPT          | 1125.628  | Assimilatory sulfite reductase (ferredoxin) [ <i>Arthrospira platensis</i> C1] (592–601)  | 1.34       |
| VDYQEQPREY          | 1325.589  | Major membrane protein I [ <i>Arthrospira platensis</i> C1] (81–90)                       | 1.30       |
| GANYEDEWK           | 1110.462  | Transketolase [ <i>Arthrospira platensis</i> ] (308–316)                                  | 1.30       |

Sequence alignment showed that the peptide INSSDVQGKY was a part of a beta-subunit of allophycocyanin. This was a novel AP first be sequenced and proved with antioxidant activity. The structure of INSSDVQGKY was predicted and it was a linear peptide with a little helix (Figure 5A). In order to validate the antioxidant function of this peptide, it was synthesized. ORAC assay of the synthesized peptide was  $0.32 \pm 0.03$  mmol TE/g and slightly lower than F2 ( $0.41 \pm 0.04$  mmol TE/g) (Figure 5B). The peptide had no significant cytotoxicity on HaCaT cells within 400  $\mu$ g/mL (Figure 5C). The peptide dose-dependently reduced the intracellular ROS levels at a concentration range from 100  $\mu$ g/mL to 400  $\mu$ g/mL (Figure 5D,E). This peptide is therefore hypothesized to be the major antioxidant component of F2. The antioxidant activity of INSSDVQGKY is close to peptide PNN which was obtained from hydrolysis of phycobiliprotein by protease K [27] and may have potential applications in further study.

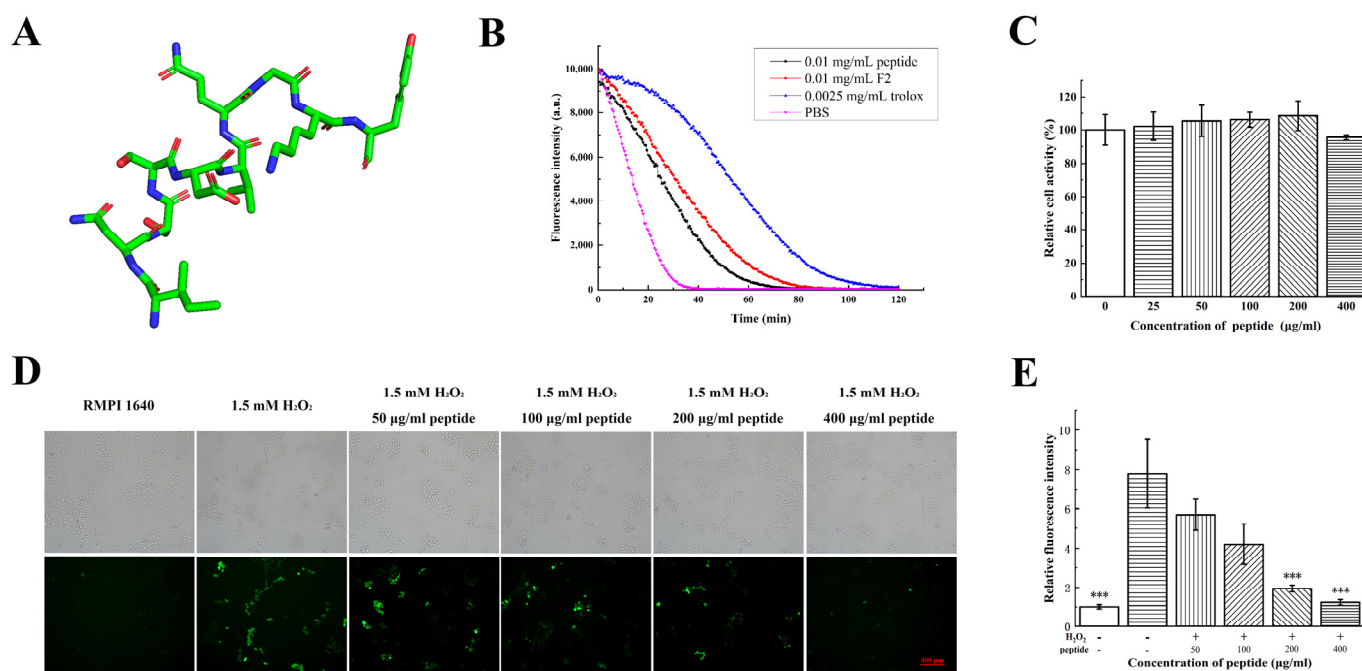


**Figure 5.** Antioxidant activities of synthesized peptide INSSDVQGKY. (A) Predicted structure of peptide INSSDVQGKY. (B) ORAC assay of synthesized peptide INSSDVQGKY compared with Trolox and PBS. (C) The effects of different concentration of synthesized peptide INSSDVQGKY on HaCaT cell viability were measured by MTT assay. (D) Antioxidant activities of synthesized peptide INSSDVQGKY on HaCaT cells were detected by DCFH-DA probe. Images were taken using fluorescence microscope (magnification, 10 $\times$ ). (E) Statistical analysis was performed to quantify relative fluorescence density. The Normality of data was analyzed by Shapiro–Wilk test. Data were expressed as mean  $\pm$  SD ( $n = 3$ ). \*\*\* represents  $p < 0.001$ , compared with H<sub>2</sub>O<sub>2</sub> group (Student  $t$ -test).

### 3. Discussion

Phycobiliprotein is an ideal marine protein resource with antioxidant properties widely spread in Rhodophyta and Cyanophyta, which could be used in bioactive peptides preparation [28]. This study aimed to apply the bacterial extracellular protease in preparing antioxidant peptides from phycobiliprotein. To utilize phycobiliprotein more comprehensively and avoid its natural limitations, we reported bacterial extracellular protease of *Pseudoalteromonas* sp. JS4–1 hydrolyzed phycobiliprotein to obtain antioxidant peptides in a single process. The bioactive fractions exhibited antioxidant activities both in vitro and in vivo. The biochemical mechanisms of the antioxidant activities of the fractions at cellular and *C. elegans* levels may be through activating the activities of antioxidant enzymes and scavenging the oxidative stress in the organisms. The molecular mechanism underlying this biological process still need to be further studied in the future.

In this study, extracellular proteases from marine bacteria were used to hydrolyze phycobiliprotein. Marine proteases can degrade organics in the ocean naturally; thus, they have extraordinary advantages in digesting marine-sourced proteins such as fish and plants compared with land proteases [9,29,30]. Compared with commercial proteases, marine proteases have higher catalyzing efficiency and shorter hydrolyzing time. The unique cleavage sites of marine proteases also produced peptides with different amino acid sequences which is helpful to select more bioactive peptides and develop various applications of phycobiliprotein [31]. The identified peptide INSSDVQGKY exhibited antioxidant activities at a concentration of 100–200  $\mu\text{g}/\text{mL}$  which was close to some newly found antioxidant peptides derived from other resources [32,33]. The cellular ROS scavenging assay is strong proof of the outstanding antioxidant activity of the peptide during biological process.

ROS are important mediators of biological process. The increased formation of ROS could cause oxidative stress which is associated with oxidative damage to biomolecules [34].

Oxidative stress happens in various pathophysiological processes and is an important pathophysiological mechanism underlying many diseases. Thus, decreasing the ROS levels to inhibit the oxidative stress has become an efficient and promising way in medicine [35]. Activating endogenous antioxidant enzymes such as SOD, CAT and GSH-Px by small molecules is an effective and protective approach in diseases [36]. The enzymatic hydrolysates and newly identified peptide in this study were able to activate the antioxidant enzymes to scavenge ROS under exogenous stress such as high glucose, and H<sub>2</sub>O<sub>2</sub>. Li G et al. identified a novel peptide EDEQKFWGK with DPPH RSA 26.76% and the OH RSA 32.19% from porcine plasma hydrolysate, and this peptide could increase SOD, CAT, and GSH-Px activities in HepG2 cells [37]. Park YR et al. identified a novel peptide NCW-PFQGVPLGFQAPP with DPPH RSA 50% from clam worms and exhibited good antioxidant and anti-inflammation effects in RAW264 7 cells [38]. Compared with antioxidant peptides from other resources, phycobiliprotein hydrolysates also showed good antioxidant activities (DPPH RSA:  $45.14 \pm 0.43\%$  and OH RSA:  $65.11 \pm 2.64\%$ ). Further, phycobiliprotein can be easily obtained and produced massively in the industry. So, exploring bioactive peptides from phycobiliprotein is of great economic value.

Conclusively, the enzymatic hydrolysis of phycobiliprotein is a promising and efficient method to produce antioxidant peptides. The peptides hydrolyzed from phycobiliprotein by marine proteases exhibited antioxidant activities both at cellular levels and in *C. elegans*.

## 4. Materials and Methods

### 4.1. Strains and Reagents

The *A. platensis* powder was purchased from a local supplier in Shanghai. Strains used in this study were isolated from the sediment of the South China Sea and stored in the lab: *Pseudoalteromonas* sp. JS4-1 (GenBank accession number: MT116988), *Pseudoalteromonas* sp. B27-3, *Pseudoalteromonas* sp. B47-6, *Pseudoalteromonas* sp. B62-3, *Pseudoalteromonas* sp. WH05-1, *Pseudoalteromonas* sp. WH06-2, and *Pseudoalteromonas* sp. ZB23-2. Immortal human umbilical vein endothelial cell line (HUVECs) and human immortal keratinocyte line (HaCaT) were obtained from the National Collection of Authenticated Cell Cultures (Shanghai, China). Wild type *C. elegans* (N2) were obtained from Caenorhabditis Genetics Center (CGC).

Ninhydrin, penicillin-streptomycin solution (cell culture grade), trypsin-EDTA solution, dimethyl sulfoxide (DMSO), thiazolyl blue tetrazolium bromide (MTT), and phosphate buffered saline (PBS) were purchased from Sangon Biotech (Shanghai, China). Trisodium citrate dihydrate, SnCl<sub>2</sub>, n-propanol, FeSO<sub>4</sub>, 30% H<sub>2</sub>O<sub>2</sub>, cholesterol and glucose were purchased from Sinopharm Chemical Reagent Co., Ltd. (Shanghai, China). In addition, 1,1-diphenyl-2-picrylhydrazyl (DPPH), 1,10-phenanthroline monohydrate (OP), fluorescein sodium salt, 2,20-azobis (2-amidinopropane) dihydrochloride (AAPH), 6-hydroxy-2,5,7,8-tetramethylchroman-2-carboxylic acid (Trolox), L-leucine, antifade mounting medium and NaN<sub>3</sub> were purchased from Sigma-Aldrich, Ltd. (St. Louis, MO, USA). Amicon™ Ultra-15 centrifugal filter units were purchased from Millipore® (Billerica, MA, USA). Sephadex LH-20 was purchased from GE Healthcare Life Sciences (Uppsala, Sweden). Fetal bovine serum (FBS) was purchased from PAN-BiotechGibco company (Aidenbach, Germany). RPMI-1640 medium was purchased from Gibco® ThermoFisher Scientific Company (Waltham, MA, USA). Methyl viologen dichloride was purchased from Aladdin® (Shanghai, China). BCA assay kit, cell lysis buffer, ROS assay kit, catalase (CAT) assay kit, total superoxide dismutase (SOD) assay kit with NBT, cellular glutathione peroxidase (GSH-Px) assay kit with NADPH and lipid peroxidation MDA assay kit were purchased from Beyotime Biotechnology (Shanghai, China).

### 4.2. Extraction of Phycobiliprotein and Screening of Proteases

#### 4.2.1. Extraction of Phycobiliprotein from *A. platensis*

One gram of *A. platensis* powder was stirred in 100 mL of sterilized ultrapure water, then frozen in  $-20\text{ }^{\circ}\text{C}$  and thawed in  $37\text{ }^{\circ}\text{C}$ -water bath repeatedly 3–4 times to help

proteins released. The protein content was measured by BCA method [39]. The soluble phycobiliprotein (crude extract) was obtained by centrifugation at  $12,000 \times g$  for 20 min, and stored at  $-20\text{ }^{\circ}\text{C}$  for future use. We could obtain 100 mL of 3.75 mg/mL protein solution from 1 g of *A. platensis* powder and the yield rate was 37.5%.

#### 4.2.2. Preparation of Crude Bacterial Extracellular Protease

The activated seed inoculum was prepared by adding bacterial strains preserved in glycerin into 5 mL 2216E liquid medium (tryptone 5 g/L, yeast extract 1 g/L,  $\text{Fe}_2(\text{SO}_4)_3$  0.01 g/L, dissolved in artificial sea water, pH 7.8), and incubating at  $16\text{ }^{\circ}\text{C}$  for 16–24 h with 180 rpm shaking. Then, 2% of seed inoculum was transformed to fresh fermentation medium (bean powder 20 g/L, corn powder 20 g/L, wheat bran 10 g/L,  $\text{Na}_2\text{HPO}_4 \cdot 12\text{H}_2\text{O}$  1 g/L,  $\text{KH}_2\text{PO}_4$  0.3 g/L,  $\text{CaCl}_2$  1 g/L,  $\text{Na}_2\text{CO}_3$  1 g/L, dissolved in artificial sea water, pH 7.8) and continuously culturing at the same condition. After 5 days cultivation, the crude enzyme was obtained by collecting the supernatant of the fermentation broth at  $12,000 \times g$  centrifugation for 10 min at  $4\text{ }^{\circ}\text{C}$ , and stored at  $-20\text{ }^{\circ}\text{C}$  prior to use.

#### 4.2.3. Substrate Immersing Zymography

Substrate immersing zymography was conducted to determine the enzymatic activities against casein according to a previous study, with minor modifications [40]. The SDS-PAGE gel was immersed in the pre-warmed 0.5% (*w/v*) casein solution and incubated at  $37\text{ }^{\circ}\text{C}$  for 1 h with 75 rpm shaking. The gel was then stained with 0.1% of Coomassie Brilliant Blue dye solution for 4 h, and then decolorized with 30% of ethanol and 70% of acetic acid (*v/v*) until the bands were clearly visible.

### 4.3. Antioxidant Activities of Hydrolysates

#### 4.3.1. Optimization of Hydrolysis Conditions

First, the enzyme/substrate (E: S) ratio (*v/w*, mL/mg) was designed as 1:6, 1:8, 1:10, 1:12 and 1:14 with 1 mg/mL enzyme at  $50\text{ }^{\circ}\text{C}$ , to optimize the E/S ratio during the hydrolyzing. Then, the hydrolysis reaction was carried out at 35 to  $60\text{ }^{\circ}\text{C}$ , with  $5\text{ }^{\circ}\text{C}$  at intervals, to estimate the optimal temperature for hydrolyzing. Finally, hydrolyzing was taken from 1 h to 7 h at hourly intervals at  $50\text{ }^{\circ}\text{C}$  to optimize the reaction time. The reaction was terminated by heating at  $95\text{ }^{\circ}\text{C}$  for 10 min. The reaction buffer was ultrapure water. The hydrolysate was centrifuged at  $12,000 \times g$  and  $4\text{ }^{\circ}\text{C}$  for 20 min and the hydrolysis degree was measured by ninhydrin coloration method [41]. The  $\bullet\text{NH}_2$  in hydrolysate could react with ninhydrin and have absorption peak at 570 nm. The standard curve was determined using L-leucine at a concentration of 0, 1, 1.5, 2, 2.5 and 3 mM.

#### 4.3.2. Purification of Hydrolysates

After digestion, the hydrolysates were added into the upper casing of the Amicon<sup>TM</sup> Ultra-15 centrifugal filter units and centrifuged at  $5000 \times g$  for 30 min to separate peptides with MWCO (molecular weight cut-off)  $> 3\text{ kDa}$  (in the upper casing) and MWCO  $< 3\text{ kDa}$  (in the lower casing).

The peptides with MWCO  $< 3\text{ kDa}$  was further fractionated by NGC Scout Plus fast protein liquid chromatography (FPLC) system (Bio-Rad, USA) and a XK16/70 column ( $1.6 \times 60\text{ cm}$ ) equipped with Sephadex LH-20 gel. One mL of sample was injected into the loading loop and the column was continuously eluted with filtered ultrapure water at a flow rate of 0.75 mL/min. The protein absorbance was monitored at 220 nm with a UV detection all the time. Fractions were lyophilized and redissolved in ultrapure water at the same concentration for further assay.

#### 4.3.3. Determination of Antioxidant Activities

To evaluate antioxidant activities of hydrolytes *in vitro*, DPPH free radical scavenging activity (DPPH RSA) assay, hydroxyl free radical (OH) scavenging activity (OH RSA) assay and oxygen radical absorbance capacity (ORAC) assay were conducted according to

previous studies, with minor modifications [42–44]. The DPPH and OH radical scavenging rate were calculated.

The ORAC was defined as Trolox equivalents (mmol TE/g sample or mmol TE/mmol sample) according to the area under the curve (AUC) and calculated using the following formula:

$$\text{ORAC} = (\text{AUC}_{\text{sample}} - \text{AUC}_{\text{control}}) / (\text{AUC}_{\text{Trolox}} - \text{AUC}_{\text{control}}) \times (\text{M}_{\text{Trolox}} / \text{M}_{\text{sample}}) \quad (1)$$

where  $\text{AUC}_{\text{sample}}$ ,  $\text{AUC}_{\text{control}}$  and  $\text{AUC}_{\text{Trolox}}$  were the integral areas under the fluorescence decay curve of the sample, PBS and Trolox, and  $\text{M}_{\text{Trolox}}$  and  $\text{M}_{\text{sample}}$  were the concentrations of the Trolox and sample, respectively.

#### 4.3.4. Protective Effects on Oxidative Damage of Plasmid DNA

To evaluate the protective effects of peptides on the oxidative damage of biological macromolecules (proteins and DNA), the protection effect assay was conducted according to a previous method, with minor modifications [15]. An amount of 8  $\mu\text{L}$  of pET-22b DNA, 2  $\mu\text{L}$  of  $\text{FeSO}_4$  (2 mM), 8  $\mu\text{L}$  of sample and 2  $\mu\text{L}$  of 0.1%  $\text{H}_2\text{O}_2$  were mixed in a sterilized tube and incubated at 37 °C for 10 min. For the blank, 12  $\mu\text{L}$  of sterilized water replaced other reagents incubating with the DNA. For the negative control, sample was replaced with sterilized water. For the positive control, the sample was replaced with Vitamin C (200  $\mu\text{g}/\text{mL}$ ). The reaction solution was then analyzed by 1% agarose gel electrophoresis under 120 V for 30 min.

#### 4.3.5. Determination of Intracellular ROS Levels and the Activities of Intracellular Oxidative Enzymes

HUVECs and HaCaT cells were cultured in RPMI-1640 medium with 10% FBS, 100 U/mL penicillin and 100  $\mu\text{g}/\text{mL}$  streptomycin (complete medium) at 37 °C in a humidified atmosphere of 5%  $\text{CO}_2$ . Cell viability was measured by MTT assay.

The 2',7'-dichloro-fluorescence diacetate (DCFH-DA) probe can be oxidized by ROS to produce green fluorescent materials which can be observed under fluorescence microscope. An amount of  $1 \times 10^5$  of cells were plated in a 24-well plate and incubated overnight. For the HUVECs cells, the medium was replaced with RPMI-1640 medium (without FBS instead, added 35 mM of glucose) for 24 h. For the HaCaT cells, the medium was replaced with RPMI-1640 medium (without FBS, but added 1.5 mM of  $\text{H}_2\text{O}_2$ ) for 4 h. For the blank, cells were treated with RPMI-1640 medium (without FBS). An amount of 10  $\mu\text{M}$  DCFH-DA probe was added to each well and incubated for 1 h. Cells were washed with PBS for 3 times and re-immersed in 500  $\mu\text{L}$  of PBS. Images were taken using an inverted fluorescence microscope (Axio vert. A1, Carl Zeiss, Oberkochen, Germany).

Next,  $2 \times 10^6$  of cells were plated in a 6-well plate and treated with the same condition. After incubating for 24 h, cells were washed with PBS for 3 times, then incubating with 150  $\mu\text{L}$  of cell lysis buffer for 30 min on ice. The suspension was centrifuged at  $12,000 \times g$  for 10 min at 4 °C. The protein concentration was measured by BCA method. The CAT, SOD and GSH-Px activities were determined according to the manufacturer's instructions.

#### 4.3.6. Antioxidant Activities Evaluation Using *C. elegans* Model

##### Maintenance of *C. elegans* and Lifespan Assay

N2 was cultured on nematode growth medium (NGM) plates supplied with *E. coli* OP50 as food at 20 °C. The age-synchronized *C. elegans* were prepared using the alkaline hypochlorite method according to Phaniendra et al. [45].

Fresh NGM plates were coated with *E. coli* OP50 containing a different concentration of APs (0.2 and 0.5 mg/mL) and incubated at 37 °C for 48 h to prepare the sample plates. Age-synchronized nematodes (L4 stage) were plated in blank plates and sample plates (80 worms on each plate), as Day 0 for lifespan assay. Nematodes on each plate were transferred to a new plate to avoid new-born worms and counted every day until all nematodes were dead. The survival rate was calculated.

#### Determination of ROS Levels and Activities of Antioxidant Enzymes in *C. elegans*

After 3 days of treatment on the sample plates, nematodes were collected into a M9 buffer (added 100  $\mu$ M DCFH-DA probe) and incubated at 20 °C for 30 min without light. Nematodes were washed with M9 buffer 3 times. For inverted fluorescence microscope observation, nematodes were anesthetized with 1  $\mu$ L of NaN<sub>3</sub> (25 mM) and 20  $\mu$ L of suspension was dropped onto the center of the slide, and 5  $\mu$ L of antifade mounting medium was added for observation.

The ROS accumulation was conducted according to previous studies, with minor modifications [46]. The fluorescence intensity was measured at 15 min intervals for 6 h with excitation 485 nm and emission 530 nm at 25 °C.

For intracellular proteins extraction, nematodes were ultrasonicated on ice and the suspension was centrifuged at 12,000 $\times$  *g* for 10 min at 4 °C. The protein concentration was measured by BCA method. The CAT, SOD and GSH-Px activities and MDA levels in the supernatant were determined according to the manufacturer's instructions.

#### Oxidative Stress Experiment

After 3 days of treatment, nematodes were transferred onto NGM plates supplied with 10 mM H<sub>2</sub>O<sub>2</sub> or 10 mM paraquat, and each plate with 80 worms. The number of survival nematodes was counted per 30 min intervals (the H<sub>2</sub>O<sub>2</sub> plates) and per 12 h intervals (the paraquat plates) until all the nematodes were dead [47]. The survival rate was calculated.

After 3 days of treatment, nematodes were transferred onto the fresh NGM plates (80 worms on each plate) and incubated at 35 °C for 10 h [48]. Numbers of survival nematodes were counted after the heat shock and the survival rate was calculated.

#### 4.3.7. Identification and Solid Phase Synthesis of APs

The sequence and composition of peptides in the active fractions were analyzed by liquid chromatography-mass spectrometry (LC-MS/MS) in Sangon Biotech Co., Ltd. (Shanghai, China). The LC-MS/MS was developed on an UltiMate 3000 RSLCnano system (Thermo, Waltham, MA, USA) coupled with a Q Exactive Plus HPLC-Mass Spectrometer (Thermo, Riverside County, CA, USA). The chromatographic separation was achieved using a C18 column (3  $\mu$ m, 120 Å, 100  $\mu$ m  $\times$  20 mm). The analysis was performed on a C18 analytical column (2  $\mu$ m, 120 Å, 750  $\mu$ m  $\times$  150 mm). Mobile phase A was 3% DMSO, 0.1% formic acid, and 97% H<sub>2</sub>O and mobile phase B was 3% DMSO, 0.1% formic acid, and 97% ACN. The flow rate was set as 300 nL/min. The MS data was processed with MaxQuant (V1.6.2.10) to identify detected peptides in *Arthrospira platensis* proteomics database. Peptide with maximal abundance was synthesized by solid phase synthesis in ChinaPeptides Co., Ltd. (Shanghai, China) according to the sequence information given by LC-MS/MS.

The structure of peptide was predicted by Phyre2 (<http://www.sbg.bio.ic.ac.uk/phyre2> (accessed on 20 December 2022)).

#### 4.4. Statistical Analysis

All the experiments and analysis were carried out in triplicate. The Normality of experimental data was analyzed by Shapiro–Wilk test. Normal experimental data were analyzed with by Student *t*-test. Non-parametric data were analyzed by Mann–Whitney test. Data were presented as the mean  $\pm$  standard deviation (SD) and *P* < 0.05 was considered as a statistically significant difference.

## 5. Conclusions

Algal protein resources are considered to be a huge treasury of bioactive peptides. More and more researchers are attempting to prepare novel bioactive peptides from algal protein through protease hydrolysis. In addition, novel proteases from marine bacteria also possess great potential in antioxidant peptide preparation, due to their high efficiency and low cost. In this study, phycobiliprotein was hydrolyzed by extracellular proteases from

*Pseudoalteromonas* sp. JS4-1 to produce antioxidant peptides. A novel antioxidant peptide INSSDVQGKY was separated and identified from the hydrolysates. The hydrolysates and peptide INSSDVQGKY exhibited excellent antioxidant activities both at cellular levels and in *C. elegans*.

**Supplementary Materials:** The following supporting information can be downloaded at: <https://www.mdpi.com/article/10.3390/md21020133/s1>, Figure S1: Total ion chromatography of F2; Figure S2: MS/MS of INSSDVQGKY.

**Author Contributions:** C.L.: conceptualization, methodology and validation. G.C.: writing—original draft and visualization. H.R., X.X., Y.C., C.W.: investigation. F.B.: writing—review and editing. H.H.: supervision and funding acquisition. All authors have read and agreed to the published version of the manuscript.

**Funding:** This work was supported by the National Natural Science Foundation of China (31900038 and 31500048), the Natural Science Foundation of Hunan Province, China (2021JJ30029), the Research Fund of The State Key Laboratory of Coal Resources and Safe Mining (SKLCSRSM22KF020), The Independent Exploration and Innovation project for postgraduates of Hunan Province (CX20220357, CX20220316), the Independent Exploration and Innovation project for postgraduates of Central South University (2022ZZTS0996), and the Open Sharing Fund for the Large-scale Instruments and Equipments of Central South University (CSUZC202244).

**Institutional Review Board Statement:** Not applicable.

**Informed Consent Statement:** Not applicable.

**Data Availability Statement:** The data presented in this study are available on request from the corresponding author. The data are not publicly available due to privacy.

**Conflicts of Interest:** The authors declare no conflict of interest.

## References

1. Lupatini, A.L.; Colla, L.M.; Canan, C.; Colla, E. Potential application of microalga *Spirulina platensis* as a protein source. *J. Sci. Food Agric.* **2017**, *97*, 724–732. [[CrossRef](#)] [[PubMed](#)]
2. Romay, C.; González, R.; Ledón, N.; Remirez, D.; Rimbau, V. C-phycoyanin: A biliprotein with antioxidant, anti-inflammatory and neuroprotective effects. *Curr. Protein Pept. Sci.* **2003**, *4*, 207–216. [[CrossRef](#)] [[PubMed](#)]
3. Marthandam Asokan, S.; Wang, T.; Su, W.T.; Lin, W.T. Antidiabetic Effects of a Short Peptide of Potato Protein Hydrolysate in STZ-Induced Diabetic Mice. *Nutrients* **2019**, *11*, 779. [[CrossRef](#)] [[PubMed](#)]
4. Qiao, Q.; Chen, L.; Li, X.; Lu, X.; Xu, Q. Roles of Dietary Bioactive Peptides in Redox Balance and Metabolic Disorders. *Oxid. Med. Cell Longev.* **2021**, *2021*, 5582245. [[CrossRef](#)] [[PubMed](#)]
5. Amigo, L.; Hernández-Ledesma, B. Current Evidence on the Bioavailability of Food Bioactive Peptides. *Molecules* **2020**, *25*, 4479. [[CrossRef](#)]
6. Wang, K.; Han, L.; Hong, H.; Pan, J.; Liu, H.; Luo, Y. Purification and identification of novel antioxidant peptides from silver carp muscle hydrolysate after simulated gastrointestinal digestion and transepithelial transport. *Food Chem.* **2021**, *342*, 128275. [[CrossRef](#)]
7. Chalamaiiah, M.; Dinesh Kumar, B.; Hemalatha, R.; Jyothirmayi, T. Fish protein hydrolysates: Proximate composition, amino acid composition, antioxidant activities and applications: A review. *Food Chem.* **2012**, *135*, 3020–3038. [[CrossRef](#)]
8. Lu, X.; Zhang, L.; Sun, Q.; Song, G.; Huang, J. Extraction, identification and structure-activity relationship of antioxidant peptides from sesame (*Sesamum indicum* L.) protein hydrolysate. *Food Res. Int.* **2019**, *116*, 707–716. [[CrossRef](#)]
9. Olena, Z.; Yang, Y.; TingTing, Y.; XiaoTao, Y.; HaiLian, R.; Xun, X.; Dong, X.; CuiLing, W.; HaiLun, H. Simultaneous preparation of antioxidant peptides and lipids from microalgae by pretreatment with bacterial proteases. *Bioresour. Technol.* **2022**, *348*, 126759. [[CrossRef](#)]
10. Xu, F.; Cha, Q.Q.; Zhang, Y.Z.; Chen, X.L. Degradation and Utilization of Alginate by Marine *Pseudoalteromonas*: A Review. *Appl. Environ. Microbiol.* **2021**, *87*, e0036821. [[CrossRef](#)]
11. Kou, X.; Gao, J.; Xue, Z.; Zhang, Z.; Wang, H.; Wang, X. Purification and identification of antioxidant peptides from chickpea (*Cicer arietinum* L.) albumin hydrolysates. *LWT—Food Sci. Technol.* **2013**, *50*, 591–598. [[CrossRef](#)]
12. Hou, H.; Wang, J.; Wang, J.; Tang, W.; Shaikh, A.S.; Li, Y.; Fu, J.; Lu, L.; Wang, F.; Sun, F.; et al. A Review of Bioactive Peptides: Chemical Modification, Structural Characterization and Therapeutic Applications. *J. Biomed. Nanotechnol.* **2020**, *16*, 1687–1718. [[CrossRef](#)] [[PubMed](#)]
13. Cai, S.; Lu, C.; Liu, Z.; Wang, W.; Lu, S.; Sun, Z.; Wang, G. Derivatives of gecko cathelicidin-related antioxidant peptide facilitate skin wound healing. *Eur. J. Pharmacol.* **2021**, *890*, 173649. [[CrossRef](#)] [[PubMed](#)]

14. Hseu, Y.C.; Vudhya Gowrisankar, Y.; Wang, L.W.; Zhang, Y.Z.; Chen, X.Z.; Huang, P.J.; Yen, H.R.; Yang, H.L. The in vitro and in vivo depigmenting activity of pterostilbene through induction of autophagy in melanocytes and inhibition of UVA-irradiated  $\alpha$ -MSH in keratinocytes via Nrf2-mediated antioxidant pathways. *Redox Biol.* **2021**, *44*, 102007. [[CrossRef](#)]
15. Wu, R.; Wu, C.; Liu, D.; Yang, X.; Huang, J.; Zhang, J.; Liao, B.; He, H. Antioxidant and anti-freezing peptides from salmon collagen hydrolysate prepared by bacterial extracellular protease. *Food Chem.* **2018**, *248*, 346–352. [[CrossRef](#)]
16. Zou, J.; Fei, Q.; Xiao, H.; Wang, H.; Liu, K.; Liu, M.; Zhang, H.; Xiao, X.; Wang, K.; Wang, N. VEGF-A promotes angiogenesis after acute myocardial infarction through increasing ROS production and enhancing ER stress-mediated autophagy. *J. Cell Physiol.* **2019**, *234*, 17690–17703. [[CrossRef](#)]
17. Nensat, C.; Songjang, W.; Tohtong, R.; Suthiphongchai, T.; Phimsen, S.; Rattanasinganchan, P.; Methenukul, P.; Kumphune, S.; Jiraviriyakul, A. Porcine placenta extract improves high-glucose-induced angiogenesis impairment. *BMC Complement. Med. Ther.* **2021**, *21*, 66. [[CrossRef](#)]
18. Rezaabakhsh, A.; Rahbarghazi, R.; Malekinejad, H.; Fathi, F.; Montaseri, A.; Garjani, A. Quercetin alleviates high glucose-induced damage on human umbilical vein endothelial cells by promoting autophagy. *Phytomedicine* **2019**, *56*, 183–193. [[CrossRef](#)]
19. Son, D.H.; Yang, D.J.; Sun, J.S.; Kim, S.K.; Kang, N.; Kang, J.Y.; Choi, Y.H.; Lee, J.H.; Moh, S.H.; Shin, D.M.; et al. A Novel Peptide, NicotinyI-Isoleucine-Valine-Histidine (NA-IVH), Promotes Antioxidant Gene Expression and Wound Healing in HaCaT Cells. *Mar. Drugs* **2018**, *16*, 262. [[CrossRef](#)]
20. Dong, H.; Liu, M.; Wang, L.; Liu, Y.; Lu, X.; Stagos, D.; Lin, X.; Liu, M. Bromophenol Bis (2,3,6-Tribromo-4,5-dihydroxybenzyl) Ether Protects HaCaT Skin Cells from Oxidative Damage via Nrf2-Mediated Pathways. *Antioxidants* **2021**, *10*, 1436. [[CrossRef](#)]
21. Wang, G.; Hao, M.; Liu, Q.; Jiang, Y.; Huang, H.; Yang, G.; Wang, C. Protective effect of recombinant *Lactobacillus plantarum* against H<sub>2</sub>O<sub>2</sub>-induced oxidative stress in HUVEC cells. *J. Zhejiang Univ. Sci. B* **2021**, *22*, 348–365. [[CrossRef](#)] [[PubMed](#)]
22. Lin, C.; Xiao, J.; Xi, Y.; Zhang, X.; Zhong, Q.; Zheng, H.; Cao, Y.; Chen, Y. Rosmarinic acid improved antioxidant properties and healthspan via the IIS and MAPK pathways in *Caenorhabditis elegans*. *Biofactors* **2019**, *45*, 774–787. [[CrossRef](#)] [[PubMed](#)]
23. Nakagawa, H.; Shiozaki, T.; Kobatake, E.; Hosoya, T.; Moriya, T.; Sakai, F.; Taru, H.; Miyazaki, T. Effects and mechanisms of longevity induced by *Lactobacillus gasseri* SBT2055 in *Caenorhabditis elegans*. *Aging Cell* **2016**, *15*, 227–236. [[CrossRef](#)]
24. Ayuda-Durán, B.; González-Manzano, S.; González-Paramás, A.M.; Santos-Buelga, C. *Caenorhabditis elegans* as a Model Organism to Evaluate the Antioxidant Effects of Phytochemicals. *Molecules* **2020**, *25*, 3194. [[CrossRef](#)] [[PubMed](#)]
25. Tsikas, D. Assessment of lipid peroxidation by measuring malondialdehyde (MDA) and relatives in biological samples: Analytical and biological challenges. *Anal. Biochem.* **2017**, *524*, 13–30. [[CrossRef](#)] [[PubMed](#)]
26. Shi, Y.; Meng, X.; Zhang, J. Multi- and trans-generational effects of N-butylpyridium chloride on reproduction, lifespan, and pro/antioxidant status in *Caenorhabditis elegans*. *Sci. Total Environ.* **2021**, *778*, 146371. [[CrossRef](#)] [[PubMed](#)]
27. Yu, J.; Hu, Y.; Xue, M.; Dun, Y.; Li, S.; Peng, N.; Liang, Y.; Zhao, S. Purification and Identification of Antioxidant Peptides from Enzymatic Hydrolysate of *Spirulina platensis*. *J. Microbiol. Biotechnol.* **2016**, *26*, 1216–1223. [[CrossRef](#)]
28. Pagels, F.; Guedes, A.C.; Amaro, H.M.; Kijjoa, A.; Vasconcelos, V. Phycobiliproteins from cyanobacteria: Chemistry and biotechnological applications. *Biotechnol. Adv.* **2019**, *37*, 422–443. [[CrossRef](#)]
29. Gómez-Estaca, J.; Bravo, L.; Gómez-Guillén, M.C.; Alemán, A.; Montero, P. Antioxidant properties of tuna-skin and bovine-hide gelatin films induced by the addition of oregano and rosemary extracts. *Food Chem.* **2009**, *112*, 18–25. [[CrossRef](#)]
30. Kim, S.Y.; Je, J.Y.; Kim, S.K. Purification and characterization of antioxidant peptide from hoki (*Johnius belengerii*) frame protein by gastrointestinal digestion. *J. Nutr. Biochem.* **2007**, *18*, 31–38. [[CrossRef](#)]
31. Wu, R.; Chen, L.; Liu, D.; Huang, J.; Zhang, J.; Xiao, X.; Lei, M.; Chen, Y.; He, H. Preparation of Antioxidant Peptides from Salmon Byproducts with Bacterial Extracellular Proteases. *Mar. Drugs* **2017**, *15*, 4. [[CrossRef](#)] [[PubMed](#)]
32. Fontoura, R.; Daroit, D.J.; Corrêa, A.P.F.; Moresco, K.S.; Santi, L.; Beys-da-Silva, W.O.; Yates, J.R., 3rd; Moreira, J.C.F.; Brandelli, A. Characterization of a novel antioxidant peptide from feather keratin hydrolysates. *New Biotechnol.* **2019**, *49*, 71–76. [[CrossRef](#)] [[PubMed](#)]
33. Ma, Y.; Huang, K.; Wu, Y. In Vivo/In Vitro Properties of Novel Antioxidant Peptide from *Pinctada fucata*. *J. Microbiol. Biotechnol.* **2021**, *31*, 33–42. [[CrossRef](#)] [[PubMed](#)]
34. Li, R.; Jia, Z.; Trush, M.A. Defining ROS in Biology and Medicine. *React. Oxyg Species* **2016**, *1*, 9–21. [[CrossRef](#)] [[PubMed](#)]
35. He, L.; He, T.; Farrar, S.; Ji, L.; Liu, T.; Ma, X. Antioxidants Maintain Cellular Redox Homeostasis by Elimination of Reactive Oxygen Species. *Cell Physiol. Biochem.* **2017**, *44*, 532–553. [[CrossRef](#)] [[PubMed](#)]
36. Christofidou-Solomidou, M.; Muzykantov, V.R. Antioxidant strategies in respiratory medicine. *Treat Respir. Med.* **2006**, *5*, 47–78. [[CrossRef](#)] [[PubMed](#)]
37. Li, G.; Zhan, J.; Hu, L.; Yuan, C.; Ying, X.; Hu, Y. Identification of novel antioxidant peptide from porcine plasma hydrolysate and its effect in in vitro digestion/HepG2 cells model. *J. Food Biochem.* **2022**, *46*, e13853. [[CrossRef](#)]
38. Park, Y.R.; Park, C.I.; Soh, Y. Antioxidant and Anti-Inflammatory Effects of NCW Peptide from Clam Worm (*Marphysa sanguinea*). *J. Microbiol. Biotechnol.* **2020**, *30*, 1387–1394. [[CrossRef](#)]
39. Walker, J.M. The bicinchoninic acid (BCA) assay for protein quantitation. *Methods Mol. Biol.* **1994**, *32*, 5–8.
40. Liu, D.; Yang, X.; Huang, J.; Wu, R.; Wu, C.; He, H.; Li, H. In situ demonstration and characteristic analysis of the protease components from marine bacteria using substrate immersing zymography. *Appl. Biochem. Biotechnol.* **2015**, *175*, 489–501. [[CrossRef](#)]

41. Leach, A.A. The determination of the substitution achieved at the alpha-amino, epsilon-amino and imidazole groups of proteins with special reference to derivatives of gelatin. *Biochem. J.* **1966**, *98*, 506–512. [[CrossRef](#)] [[PubMed](#)]
42. Dávalos, A.; Gómez-Cordovés, C.; Bartolomé, B. Extending applicability of the oxygen radical absorbance capacity (ORAC-fluorescein) assay. *J. Agric. Food Chem.* **2004**, *52*, 48–54. [[CrossRef](#)] [[PubMed](#)]
43. Shimada, K.; Fujikawa, K.; Yahara, K.; Nakamura, T. Antioxidative properties of xanthan on the autoxidation of soybean oil in cyclodextrin emulsion. *J. Agric. Food Chem.* **1992**, *40*, 945–948. [[CrossRef](#)]
44. Wang, B.; Li, Z.R.; Chi, C.F.; Zhang, Q.H.; Luo, H.Y. Preparation and evaluation of antioxidant peptides from ethanol-soluble proteins hydrolysate of *Sphyrna lewini* muscle. *Peptides* **2012**, *36*, 240–250. [[CrossRef](#)]
45. Alugoju, P.; Janardhanshetty, S.S.; Subaramanian, S.; Periyasamy, L.; Dyavaiah, M. Quercetin Protects Yeast *Saccharomyces cerevisiae* pep4 Mutant from Oxidative and Apoptotic Stress and Extends Chronological Lifespan. *Curr. Microbiol.* **2018**, *75*, 519–530. [[CrossRef](#)]
46. Lin, C.; Su, Z.; Luo, J.; Jiang, L.; Shen, S.; Zheng, W.; Gu, W.; Cao, Y.; Chen, Y. Polysaccharide extracted from the leaves of *Cyclocarya paliurus* (Batal.) Iljinskaja enhanced stress resistance in *Caenorhabditis elegans* via *skn-1* and *hsf-1*. *Int. J. Biol. Macromol.* **2020**, *143*, 243–254. [[CrossRef](#)]
47. Sakamoto, T.; Imai, H. Hydrogen peroxide produced by superoxide dismutase SOD-2 activates sperm in *Caenorhabditis elegans*. *J. Biol. Chem.* **2017**, *292*, 14804–14813. [[CrossRef](#)]
48. Yasuda, K.; Kubo, Y.; Murata, H.; Sakamoto, K. Cortisol promotes stress tolerance via DAF-16 in *Caenorhabditis elegans*. *Biochem. Biophys. Rep.* **2021**, *26*, 100961. [[CrossRef](#)]

**Disclaimer/Publisher’s Note:** The statements, opinions and data contained in all publications are solely those of the individual author(s) and contributor(s) and not of MDPI and/or the editor(s). MDPI and/or the editor(s) disclaim responsibility for any injury to people or property resulting from any ideas, methods, instructions or products referred to in the content.